

# CONSTRAINED OPTIMAL CONTROL OF A SPHERICAL PARALLEL MANIPULATOR

AVIRAM YANOVER

DANIEL CHOUKROUN

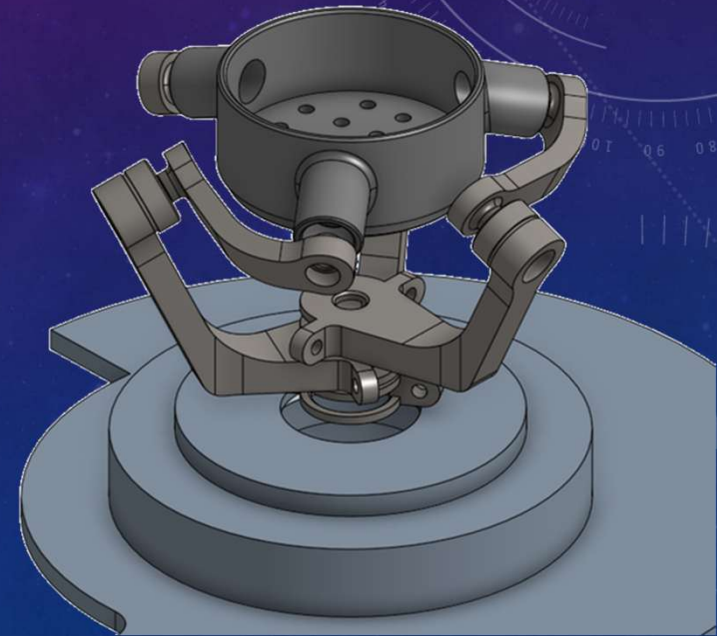
BEN GURION UNIVERSITY OF THE NEGEV

MECHANICAL ENGINEERING DEPARTMENT

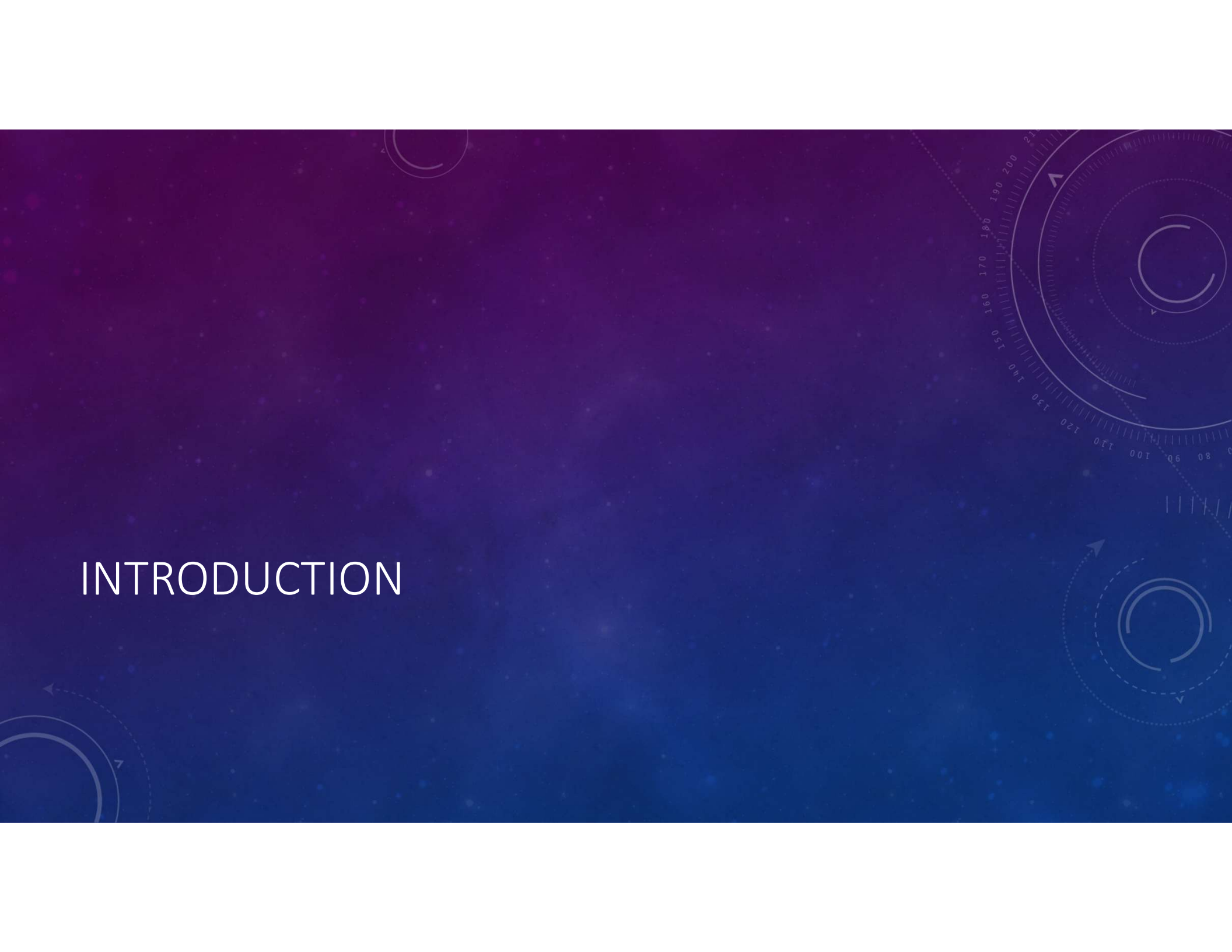
2025 IAAC Control Conference (IAAC3), Apr 28<sup>th</sup>, 2025, Hertzelia

# OUTLINE

- Introduction
- Plant model
- Controller designs & Rest-to-Rest Simulation Results
- Target Tracking
- Discussion



# INTRODUCTION

The background is a gradient from dark purple to dark blue, filled with a field of small, light-colored stars. On the right side, there are several technical diagrams. The most prominent is a large circular gauge with a scale from 0 to 210, with major markings every 10 units. It has a dashed outer ring and a solid inner ring. Below it is another circular diagram with a dashed outer ring and a solid inner ring, with an arrow pointing clockwise. In the bottom left corner, there is a partial circular diagram with a dashed outer ring and a solid inner ring, with an arrow pointing clockwise. In the top left corner, there is a partial circular diagram with a dashed outer ring and a solid inner ring, with an arrow pointing clockwise.

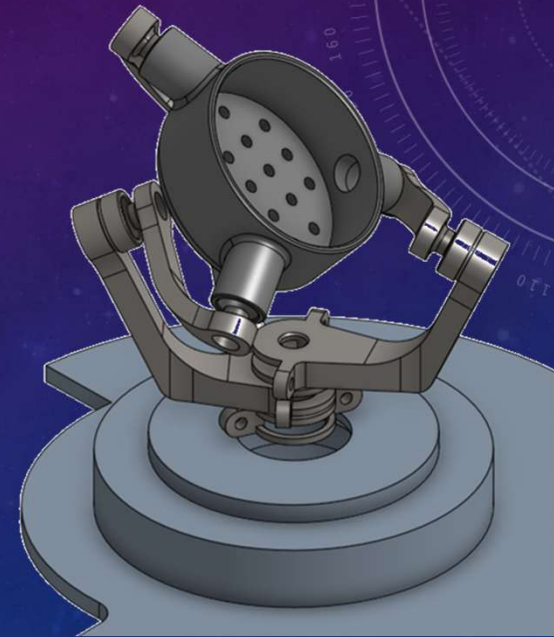
# INTRODUCTION

- A mechanism for rotating a platform around a fixed center
- The links and platform form a kinematic loop
- Belongs to the family of parallel robots
- We wish to find the best sequence of control inputs that rotates the platform from any initial position to point at a desired line of sight (rest-to-rest).



## INTRODUCTION (CONT.)

- Trajectories are expected to be short
- Limited on-board computing power
- Perturbations in sensing and actuation
- Loss of controllability due to singularities
- Simple feedback-based control is fast and geometrically intuitive but not always safe.
- Model-Predictive Control is computationally intensive



# THE PLANT MODEL

The background features a gradient from dark purple to deep blue, overlaid with a field of small white stars. On the right side, there are several technical diagrams: a large circular gauge with numerical markings from 80 to 210, a smaller circular diagram with concentric lines and arrows, and a dashed circular path with an arrow. In the bottom left corner, there are partial views of similar circular diagrams.

# THE PLANT

- Initial inverse kinematics
- Forward kinematics
- Singularity and collision monitoring

$$\dot{Q} = [\omega \times] Q$$

$$\dot{\theta} = \gamma$$

$$\omega = J_{DK}(Q, \theta) \gamma$$

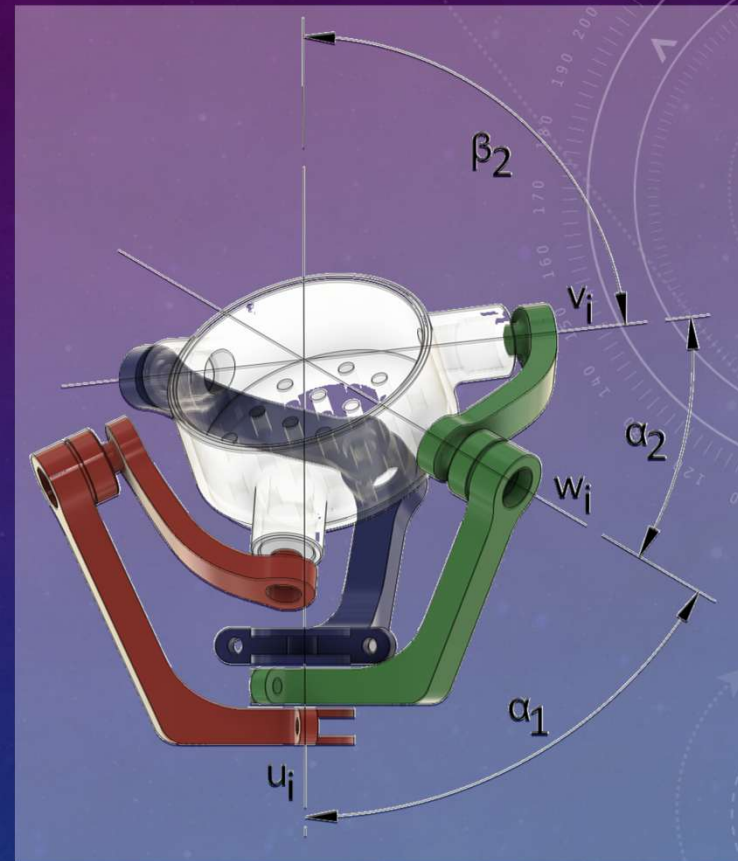
$$J_{DK}(Q, \theta) = -A^{-1}B$$

$Q$  – Platform's Rotation Operator

$\theta$  - Joint Angles

$\omega$  – Platform's Angular Velocity

$\gamma$  – Command Joint Rates

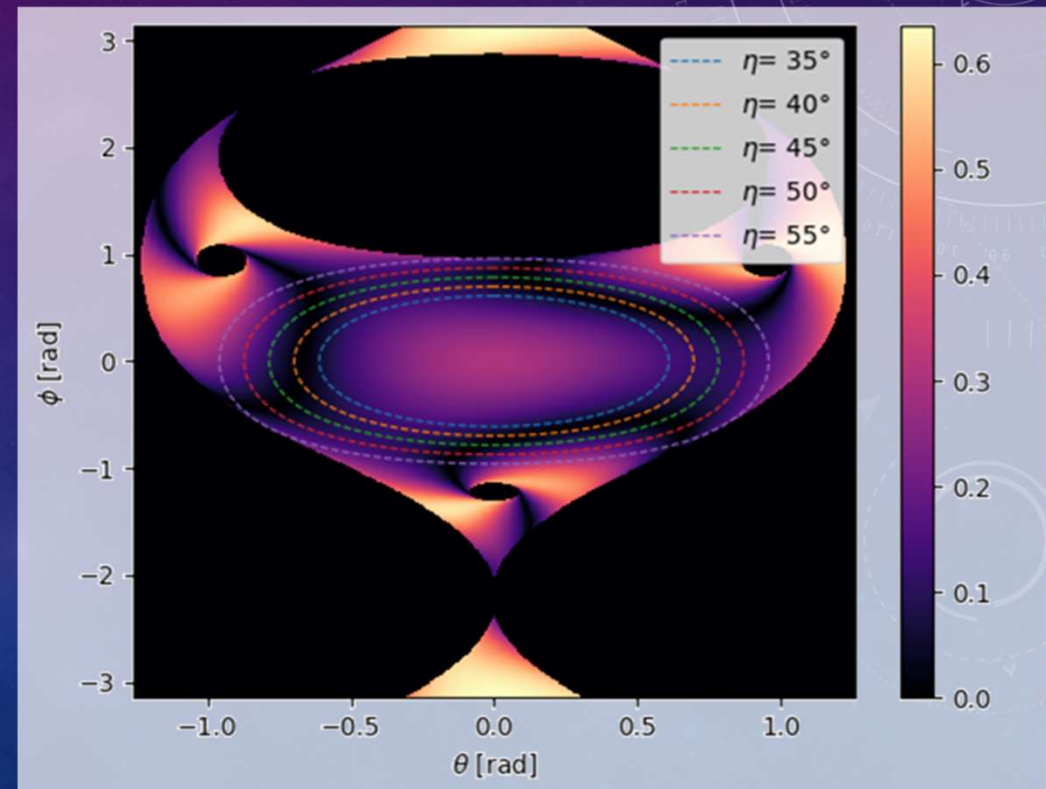


$$A = \begin{bmatrix} (w_1 \times v_1)^T \\ (w_2 \times v_2)^T \\ (w_3 \times v_3)^T \end{bmatrix}$$

$$B = \text{diag}(w_1 \times u_1 \cdot v_1, w_2 \times u_2 \cdot v_2, w_3 \times u_3 \cdot v_3)$$

## 2<sup>ND</sup> KIND SINGULARITY VS CO-ELEVATION CONTOURS

- $\text{Det}(A)$  as a function of  $\phi$  and  $\theta$
- Singularity zones in black color
- Contours correspond to different elevation angles



# CONTROLLER DESIGN

The background features a dark blue gradient with a field of small white stars. On the right side, there are several technical diagrams: a large circular scale with numerical markings from 80 to 210, a smaller circular diagram with concentric circles and arrows, and another circular diagram with dashed lines and arrows. In the bottom left corner, there are partial circular diagrams with arrows.

# QUATERNION FEEDBACK CONTROL

- Inspired by satellite attitude control
- Quaternion kinematics

$$\dot{q} = -\frac{1}{2} \begin{bmatrix} [e \times] + qI_3 \\ -e^T \end{bmatrix} \omega$$
$$\omega = J_{DK}(Q, \theta) \gamma$$

- Command joint rates

$$\gamma = -K(B^{-1}A)e$$

- Non-linear regulator, globally convergent, Lyapunov analysis
- Geometrically intuitive, LQ optimal
- Unconstrained (UF)

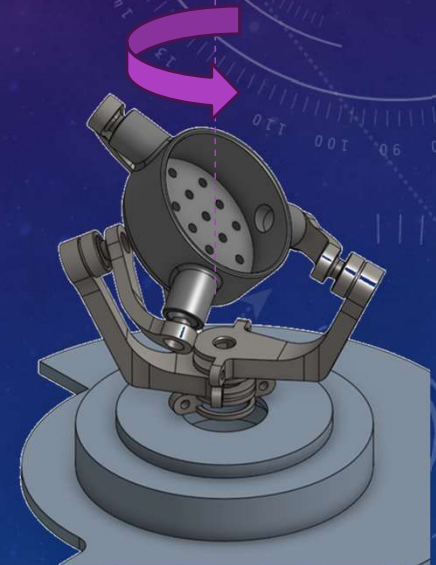
## PROPOSED APPROACH

- Separation of Elevation and Azimuth control
  - Elevation control via advanced computational methods
  - Azimuth control via proportional feedback with saturation

$$\gamma(t) = \gamma_{EL}(t) + \gamma_{AZ}(t)$$

# AZIMUTH CONTROLLER

- Azimuth control is designed as a proportional control with azimuth error feedback.
- Identical command rates are applied to the three joints.
- The joint rate command is limited by the joint maximum speed trimmed with the rates allocated to the elevation control.



# ELEVATION CONTROLLER

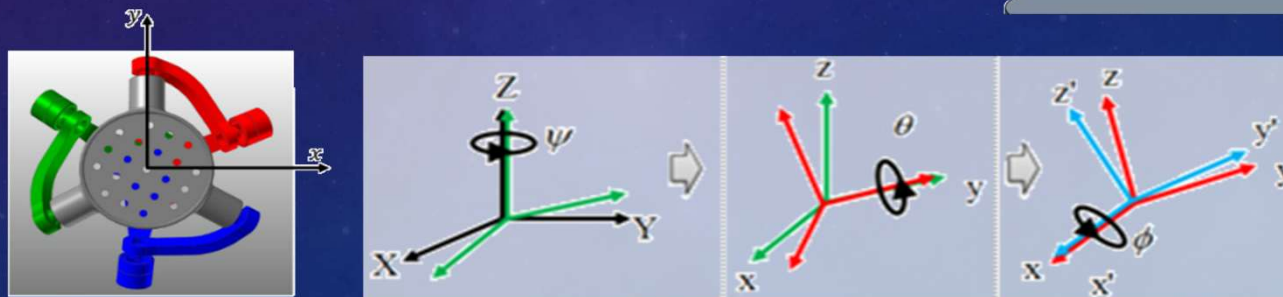
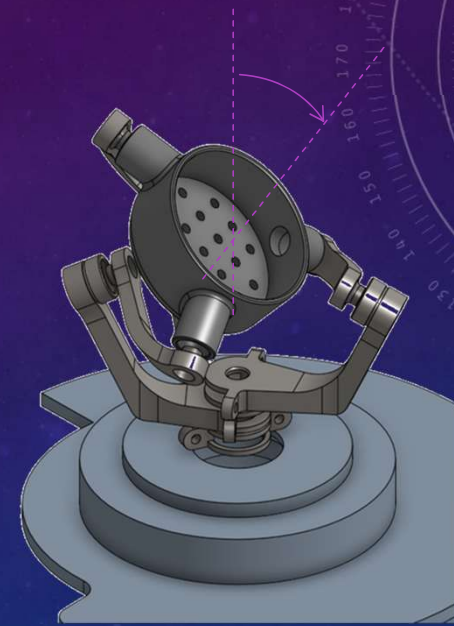
- Reinforcement Learning Approach
- Grid Search Approach

# REINFORCEMENT LEARNING METHOD

The background is a dark blue gradient with a starry or particle-like texture. On the right side, there are several circular elements: a large scale with numbers from 80 to 210, and several smaller concentric circles with arrows indicating a clockwise direction.

# ELEVATION DRL CONTROL

- Euler angles, 3-2-1 sequence, Base to Platform
- Two methodologies:
  - A2C (Discrete action space)
  - TD3 (Continuous action space)
- Stable-Baselines3\* package in Python



\* <https://stable-baselines3.readthedocs.io/en/master/#>

# ELEVATION DRL CONTROL

- The action space for A2C encompasses a finite number of discrete actions.
- For TD3, the action space is continuous, allowing for any joint rate within the range of  $-400$  to  $400$  degrees per second.
- Episodes initiate from a randomly determined state within a predefined bounding cone.
- Episodes conclude in one of three conditions:
  - The platform aligns with the desired line of sight within an error tolerance,
  - The platform exceeds a singularity threshold of  $0.05$ ,
  - The episode surpasses  $400$  steps.



# ELEVATION DRL CONTROL - THE REWARD FUNCTION

- The reward function is formulated as

$$R(s_t, a_t, s_{t+1}) = T(s_{t+1}) + F(s_t, a_t, s_{t+1})$$

- $T(s_{t+1})$  is the terminal outcome:

$$T(s_{t+1}) = \begin{cases} 50, & \text{if target reached} \\ -70, & \text{if singularity threshold exceeded} \end{cases}$$

- $F(s_t, a_t, s_{t+1})$  is an immediate outcome:

$$F(s_t, a_t, s_{t+1}) = 10(\gamma_{A_{t+1}} - \gamma_{A_t}) + 30(\eta_t - \eta_{t+1}) - 0.2$$

$\gamma_{A_t}$  denote the singularity index  $\det(A_t)$  at step  $t$

$\eta_t$  denote the elevation error at step  $t$

# TRAINING

| Alg.              | A2C           | TD3         |
|-------------------|---------------|-------------|
| Action Space      | Discrete      | Continuous  |
| N                 | 400           |             |
| $\dot{\theta}_s$  | 100, 200, 400 | [-400, 400] |
| $\tau$            | 0.05          |             |
| $\epsilon$        | 0.2°          |             |
| $\vartheta_{max}$ | 40°, 55°      |             |
| $\alpha$          | $7e - 4$      |             |
| $\gamma$          | 0.99          |             |
| $\alpha_1$        | 65°           |             |
| $\alpha_2$        | 60°           |             |
| $\beta_1$         | 0°            |             |
| $\beta_2$         | 110°          |             |

Max. no of steps

Angular velocity [°/sec]

Singularity threshold

Tolerance for reaching the target

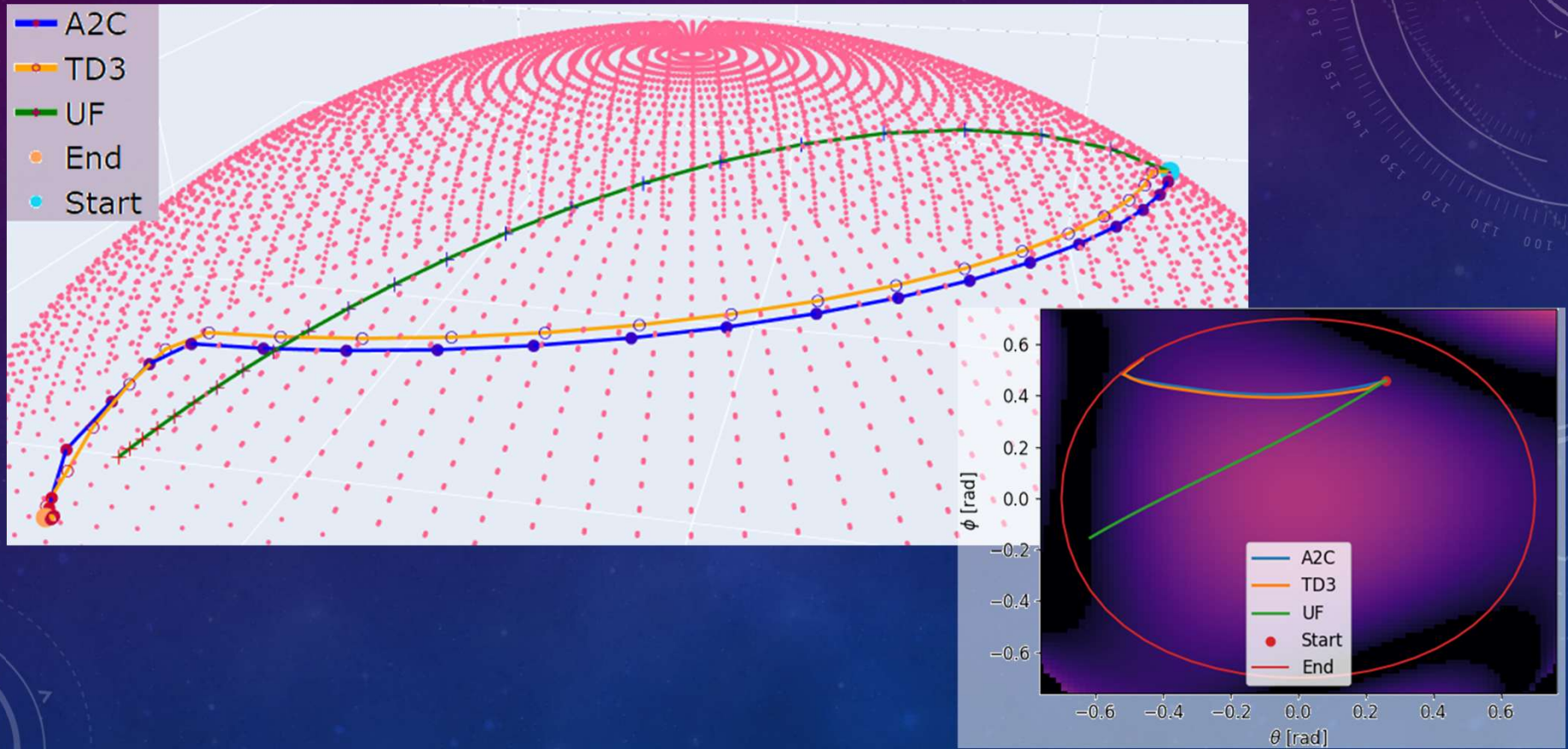
Bounding cone angle

Learning rate

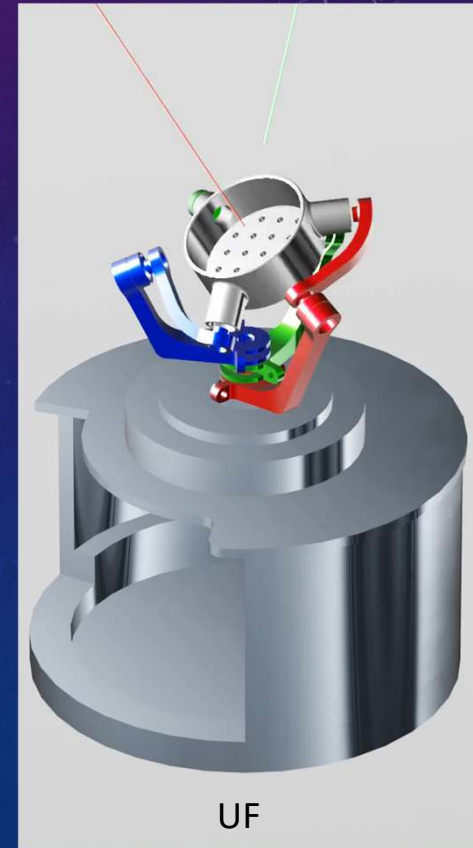
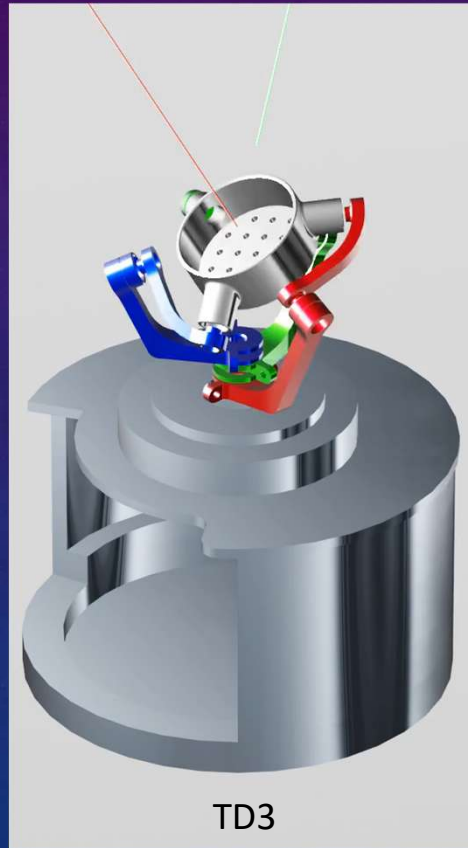
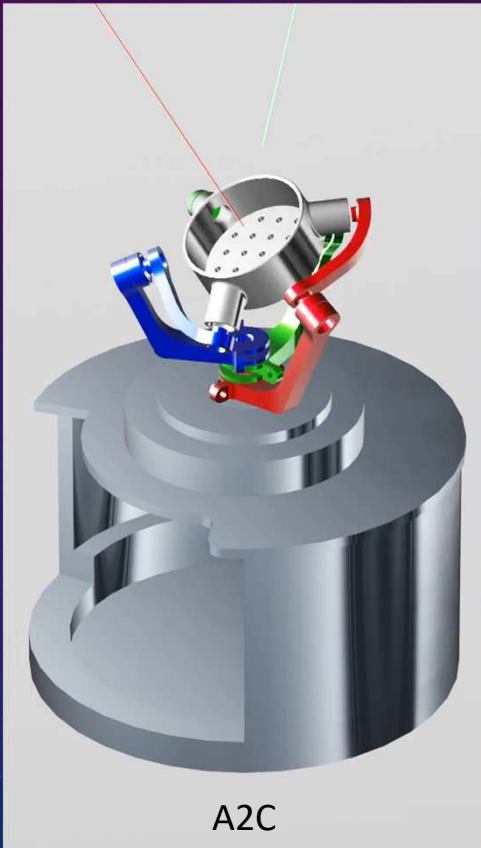
Discount factor

SPM geometry

# RL TRAJECTORIES

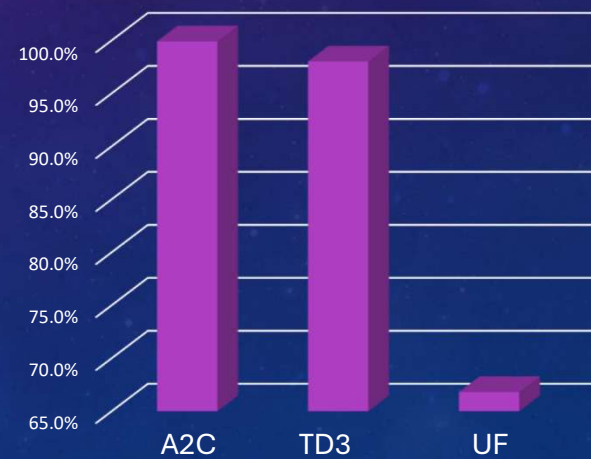


# ANIMATION



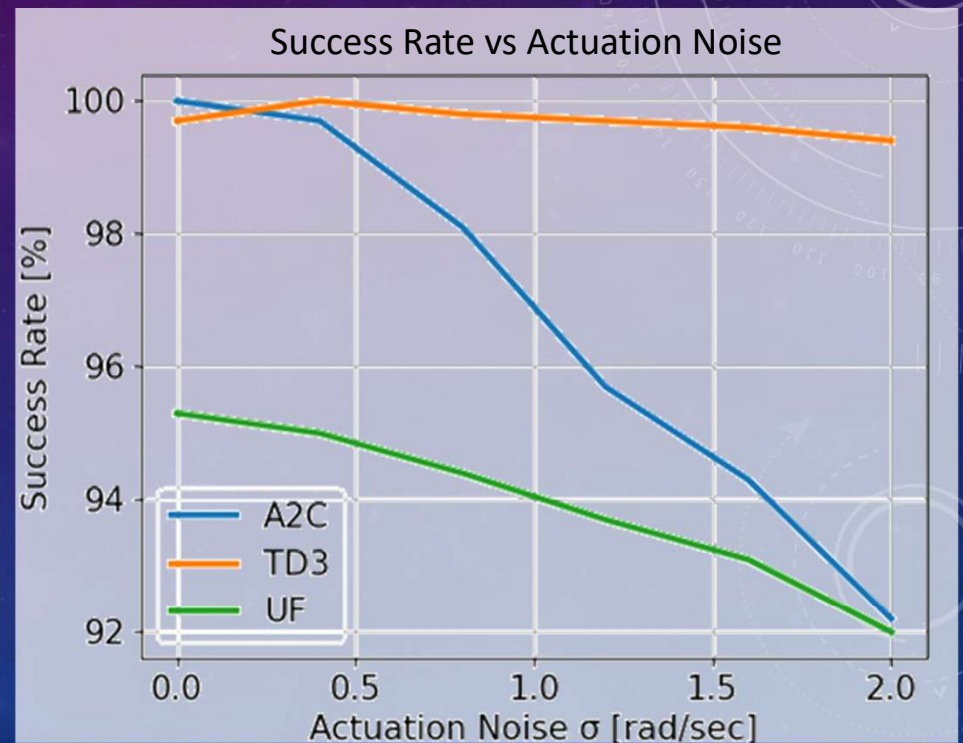
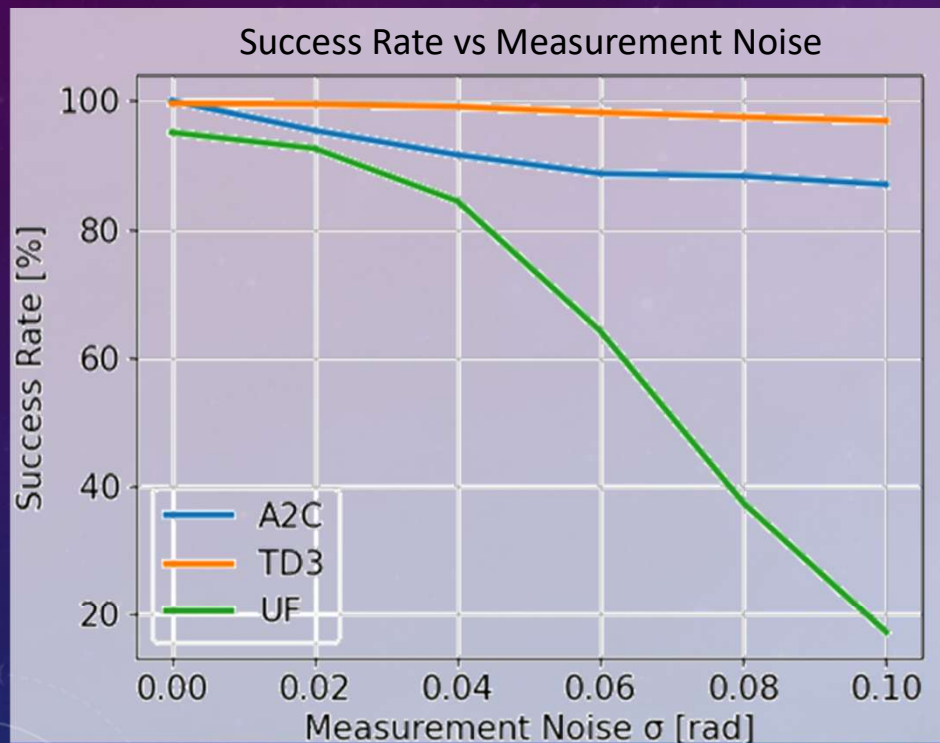
# DRL SIMULATION RESULTS SENSITIVITY TO LOS BOUNDARIES

|                     | A2C  | TD3        | UF    | A2C   | TD3         | UF    |
|---------------------|------|------------|-------|-------|-------------|-------|
| Source El. Range    |      | (0° - 40°) |       |       | (0° - 40°)  |       |
| Target El. Range    |      | (0° - 40°) |       |       | (35° - 40°) |       |
| Success rate        | 100% | 99.7%      | 95.3% | 99.9% | 98%         | 66.8% |
| Average Arc Length* | 50°  | 47°        | 33°   | 76°   | 66°         | 42°   |

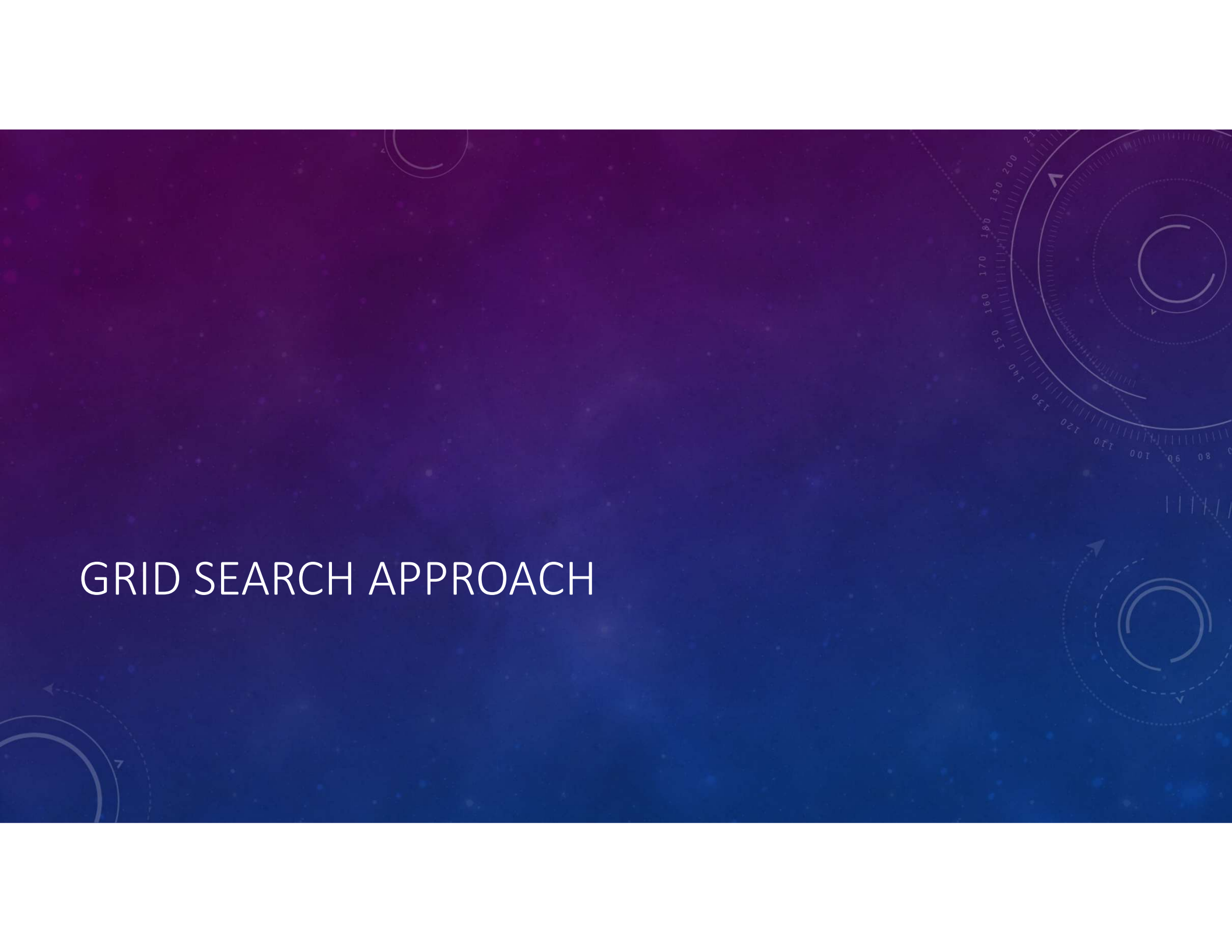


\* Successful episodes only

# SENSITIVITY TO NOISES (0°-40°)



# GRID SEARCH APPROACH

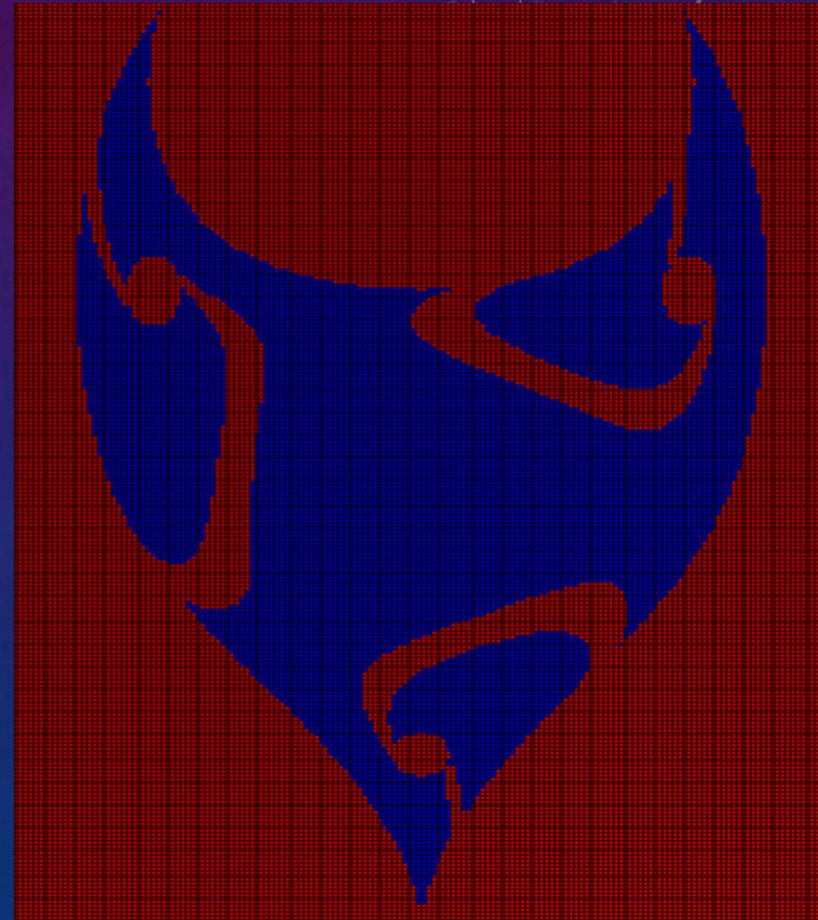
The background features a dark blue gradient with faint, light blue circular patterns and a large, detailed circular scale on the right side. The scale has numerical markings from 0 to 210 in increments of 10, with a central circular element and an arrow pointing upwards. The overall aesthetic is technical and futuristic.

# SINGULARITY MAP DISCRETIZATION

- The singularity map is constructed as a discretized grid of cells in the  $\phi$ - $\theta$  plane.
- Each grid cell corresponds to a small region.
- The singularity status of each cell is determined by sampling points :

$$S_{ij} = \begin{cases} 0 & \text{if any sampled point in the cell is singular,} \\ 1 & \text{otherwise (singularity - free)} \end{cases}$$

- Step size is determined by the cell size.



# CONTROL ALGORITHM

- **Step 1:** Obtain the current manipulator position in Euler angles  $(\phi_S, \theta_S)$ .
- **Step 2:** Get the target position relative to the manipulator.
- **Step 3:** Choose a target solution  $(\phi_T, \theta_T)$  among all feasible  $\phi$ - $\theta$  positions pointing to the target elevation, using one of two methods:

- Furthest-from-singularity method

$$(\phi_T, \theta_T) = \arg \max_{(\phi, \theta)} (\text{distance to singular points})$$

- Closest-to-source method

$$(\phi_T, \theta_T) = \arg \min_{(\phi, \theta)} \|(\phi, \theta) - (\phi_S, \theta_S)\|_2$$

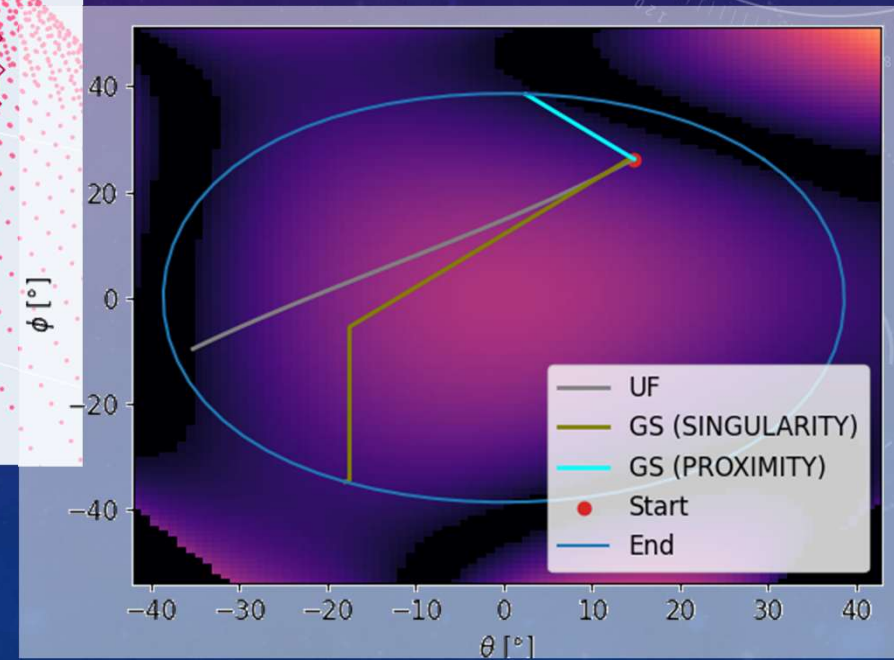
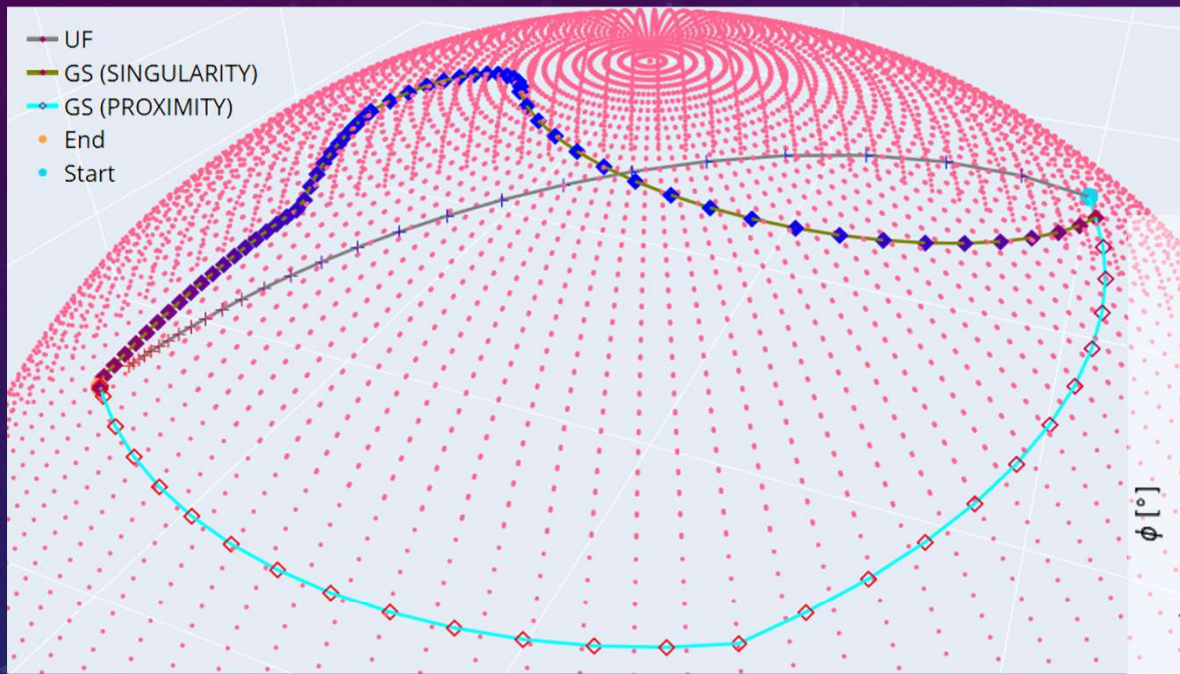
# CONTROL ALGORITHM (CONT.)

- **Step 4: Calculate a feasible path using some grid search algorithm (Dijkstra, A\*, Greedy, Beam Search, etc.)**
- **Step 5: Follow the path to the target's cell using inverse kinematics, from one cell to the next, then move directly to the target,**

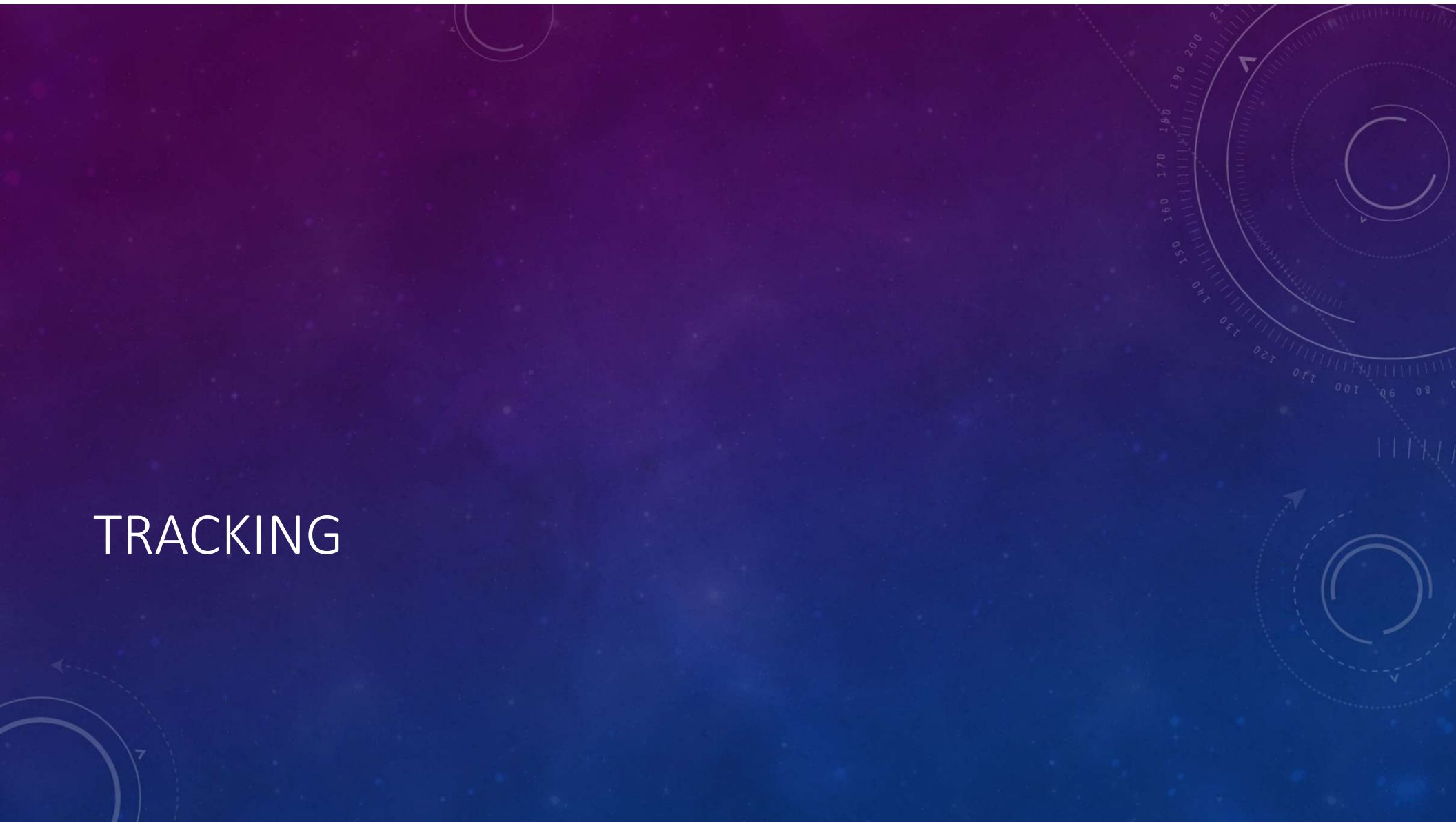
**Or:**

- **Repeat (for tracking a moving target)**
  - **At each control cycle k:**
    - **Update the Platform's current position  $(\phi_S^k, \theta_S^k)$**
    - **Update the target's current position  $(\phi_T^k, \theta_T^k)$**
    - **Recalculate the path with an appropriate singularity map**
      - Coarse resolution for long trajectories.
      - Fine resolution for refinements near the target.
    - **Move to the next cell or directly to the target**

# GRID SEARCH TRAJECTORIES



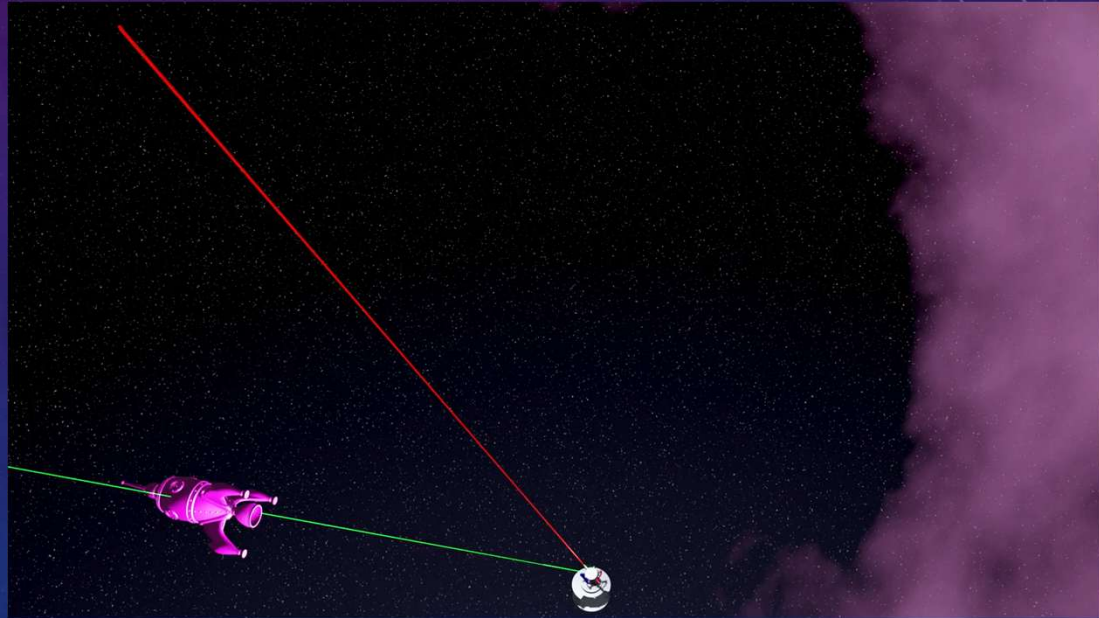
# TRACKING



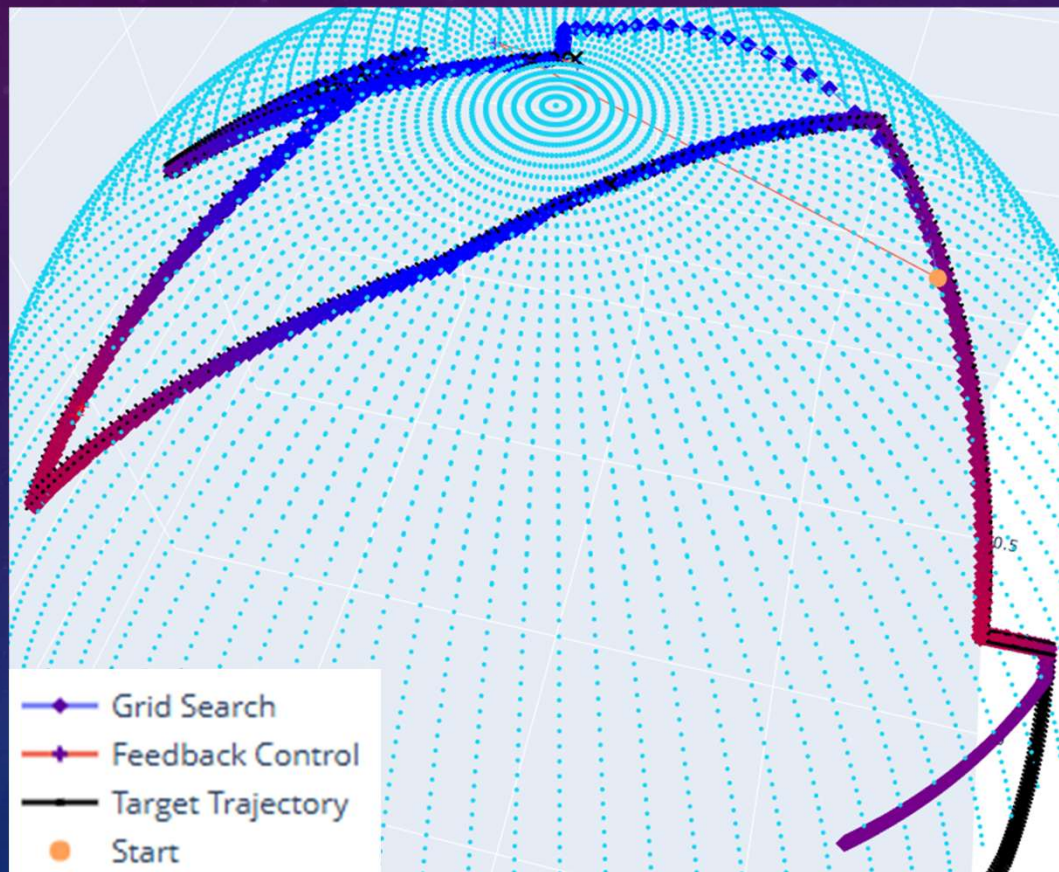
Seed=42

# RANDOM LINEAR TARGET

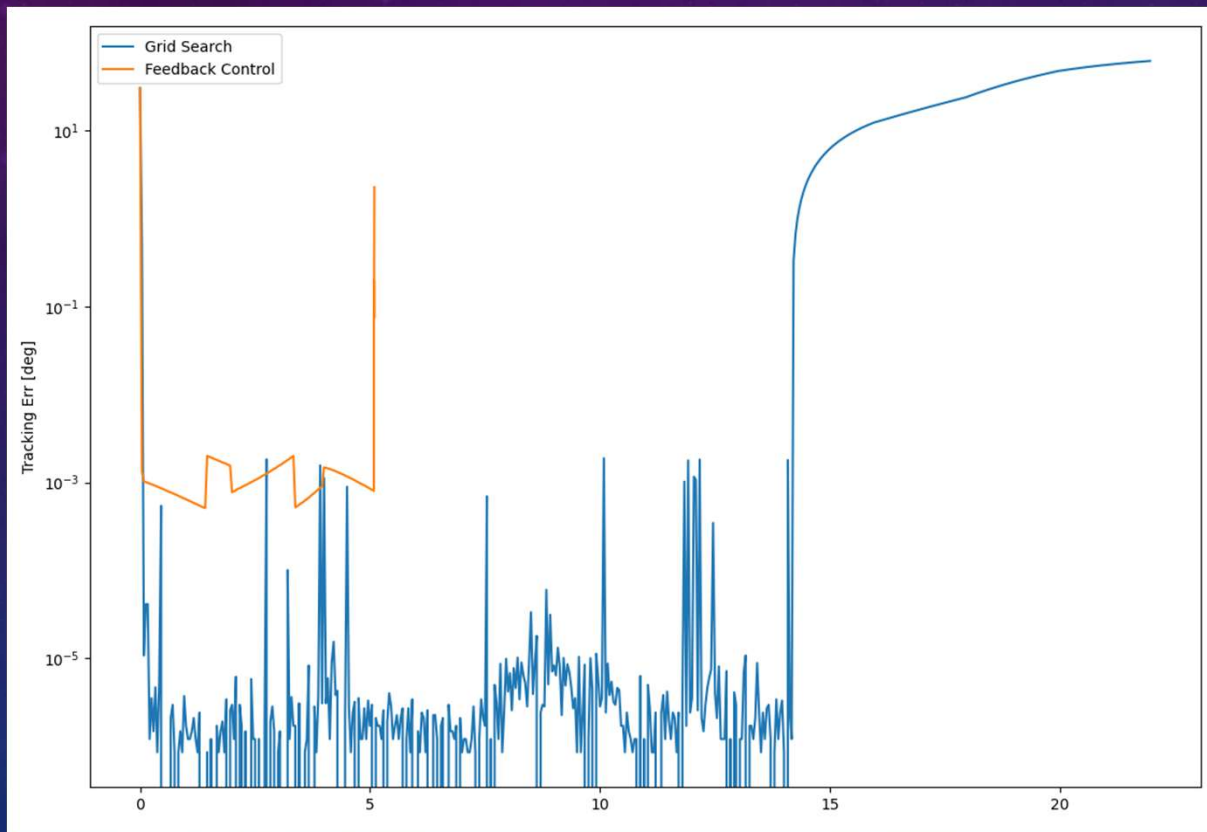
- Tracking Time = 22sec
- Duration for which the point moves in a single random direction before potentially changing its direction = 2sec
- Speed = 50m/sec
- Sampling Freq. = 24hz
- $p_0 = (10, 0, 100) m$



# RANDOM LINEAR TARGET TRACKING LOS



# RANDOM LINEAR TARGET TRACKING ERROR



# RANDOM LINEAR TARGET TRACKING ANIMATION

Grid Search

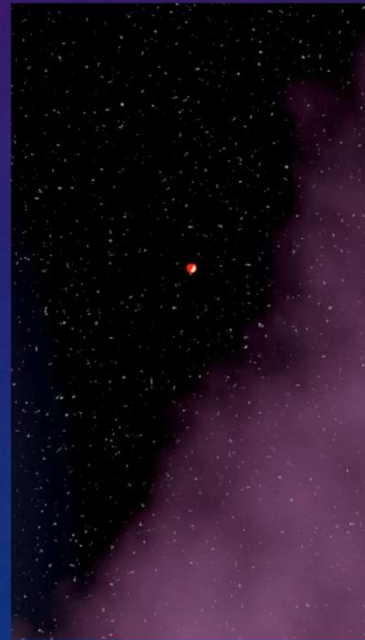
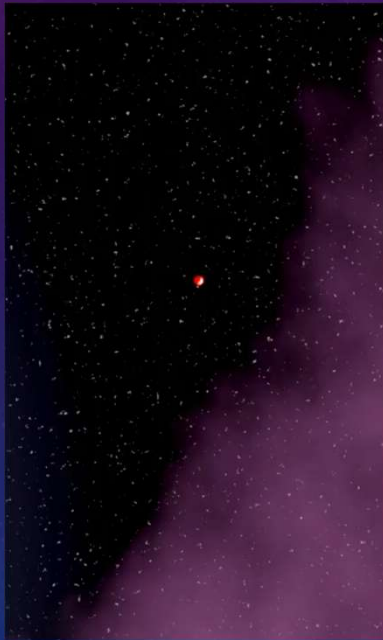
Unconstrained Feedback Control



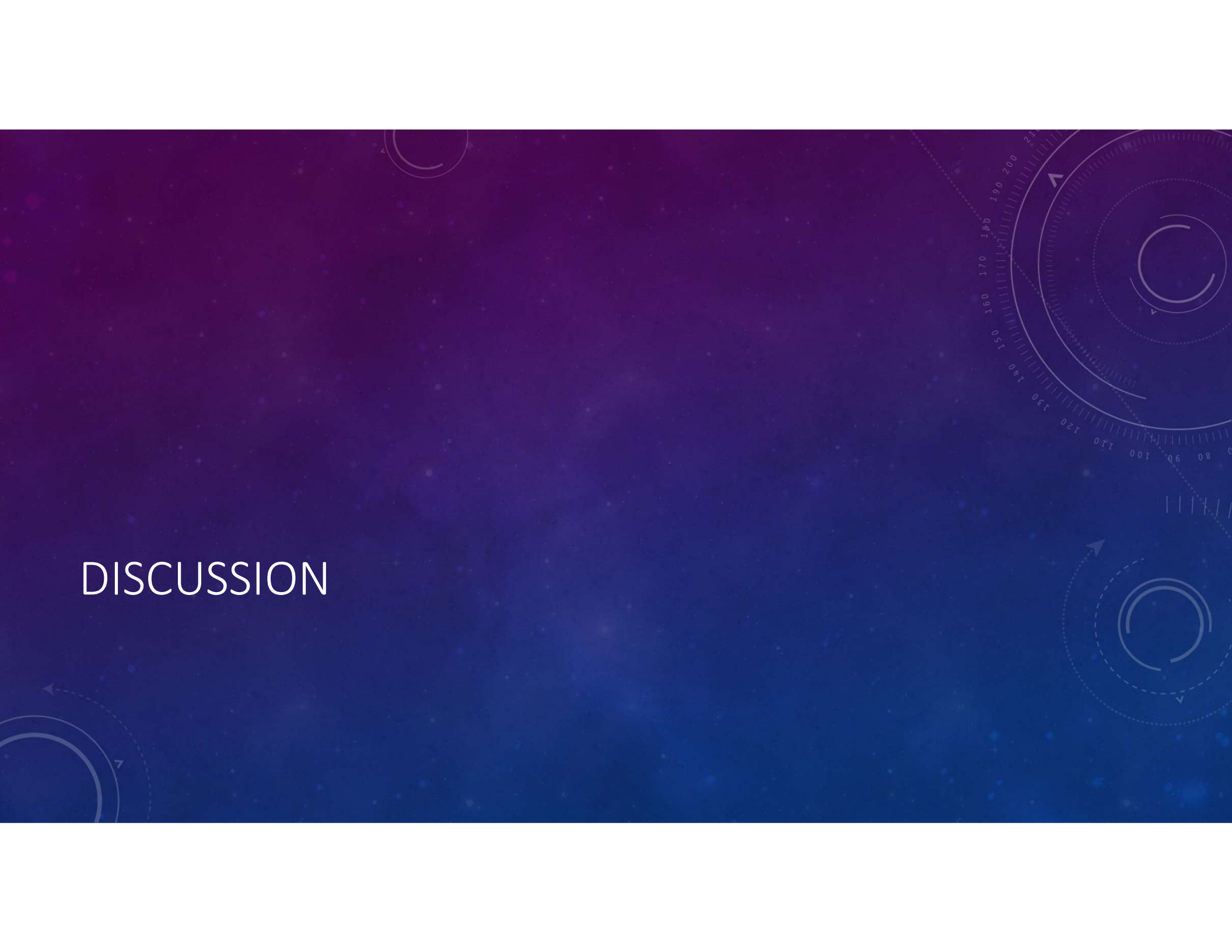
# RANDOM LINEAR TARGET TRACKING ANIMATION

Grid Search

Unconstrained Feedback Control



# DISCUSSION



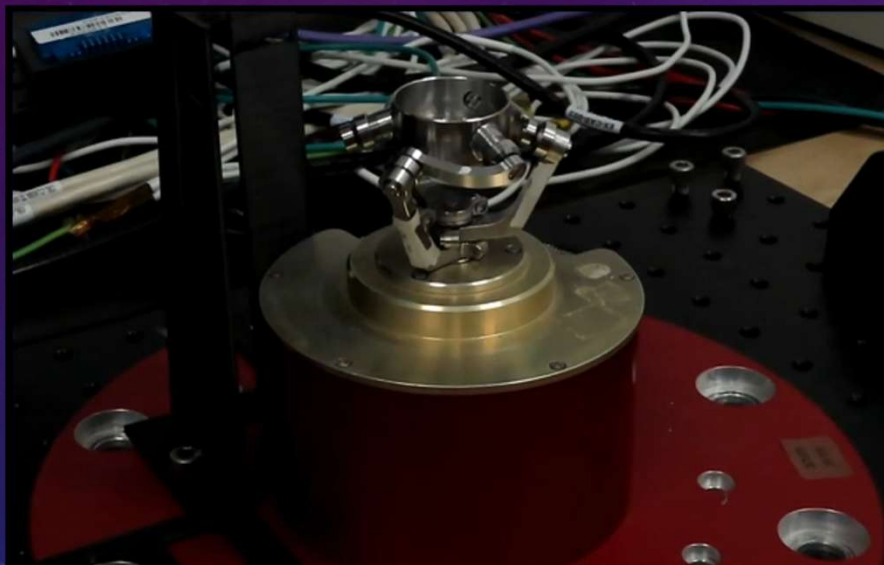
# DISCUSSION – PROS & CONS

| RL (Discrete Actions)   | Grid Search  | Unconstrained Feedback Control   |
|---|--|--|
| <p>Pros:</p> <ul style="list-style-type: none"><li>• Robustness</li><li>• Efficiency</li><li>• High Success Rates</li></ul> <p>Cons:</p> <ul style="list-style-type: none"><li>• Pre-Training Overhead</li><li>• Non-Deterministic Behavior</li><li>• Reduced Maneuverability</li></ul> | <p>Pros:</p> <ul style="list-style-type: none"><li>• Deterministic</li><li>• No Pre-Training</li><li>• Safety &amp; Reliability</li></ul> <p>Cons:</p> <ul style="list-style-type: none"><li>• Computational Toll</li><li>• Path Optimality</li><li>• Smoothness</li><li>• Reduced Maneuverability</li></ul> | <p>Pros:</p> <ul style="list-style-type: none"><li>• Simplicity</li><li>• Shortest Trajectories</li><li>• Low Computational Cost</li><li>• High Maneuverability</li></ul> <p>Cons:</p> <ul style="list-style-type: none"><li>• Lack of Singularity Avoidance</li><li>• Limited Robustness</li><li>• Tracking Limitations</li></ul> |

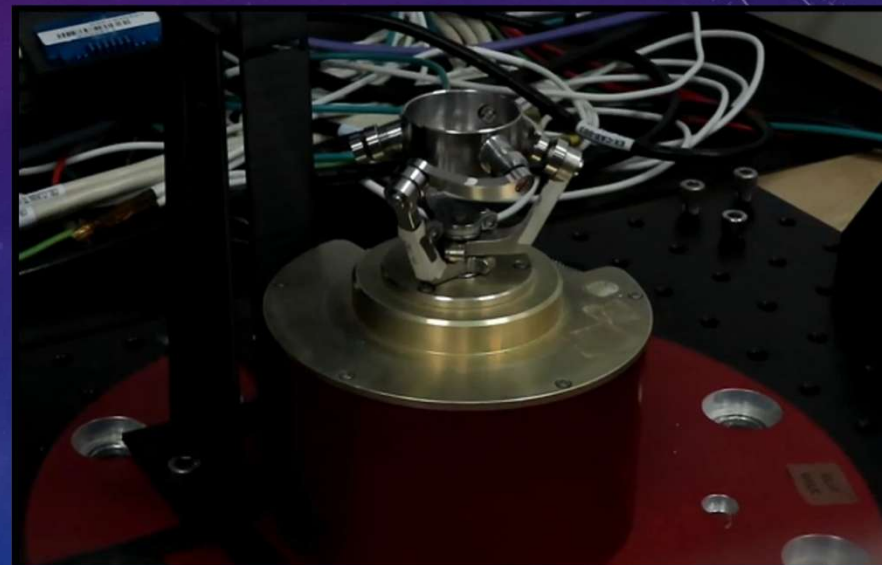
# DISCUSSION - INSIGHTS AND FUTURE DIRECTIONS

- The reduced maneuverability in RL and Grid Search approaches is a trade-off for their safety and reliability.
- The unconstrained method excels in smooth and efficient motion but struggles with singularity avoidance at high elevation angles.
- The RL model, being a lightweight neural network, is well-suited for deployment on low-power hardware such as ASICs.
- The grid search approach requires CPU resources for real-time pathfinding and command conversion.
- The multi-resolution approach in Grid Search reduces computational costs, making its real-time performance comparable to RL inference.
- Hybrid approaches could leverage the strengths of the unconstrained method with RL or Grid Search to achieve optimal control.

# RL DEMO EXPERIMENT



A2C



TD3